Solar Physics (2006) 233: 129–138
DOI: 10.1007/s11207-006-2099-5

INTERFERENCE MECHANISM OF "ZEBRA-PATTERN" FORMATION IN SOLAR RADIO EMISSION

V. G. LEDENEV
Institute of Solar-Terrestrial Physics SB RAS, P.O. Box 4026, Irkutsk 664033, Russia
(e-mail: leden@iszf.irk.ru)

and

Y. YAN and Q. FU
National Astronomical Observatories, Beijing 100012, China

(Received 23 May 2005; accepted 28 October 2005)

Abstract. It is shown that "zebra-pattern" in solar continuum events (in type IV bursts) can be formed as a result of interference between direct and reflected rays coming from a source of small size in a stratified atmosphere. The emission is generated by plasma mechanism. Full emission flux is contributed from a great number of narrow-band short-lived sources of small sizes, which are formed by plasma waves captured in density minima of background plasma fluctuations.

1. Introduction

Powerful solar flares are usually accompanied by broad-band radio continua (type IV bursts) (Kundu, 1965; Zheleznyakov, 1970; Krüger, 1979), and against their background the so-called "zebra-patterns" are frequently observed (Figures 1 and 2). They show up as a number (up to 10 and more) of almost parallel and equidistant stripes (Elgarøy, 1959; Slottje, 1972). Most often, such structures are observed in meter and decimeter ranges (Chernov, 1976; Izliker and Benz, 1994). Sometimes such structures are observed in the microwave emission (Ning, Fu, and Lu, 2000; Ledenev *et al.*, 2001; Ledenev, Yan, and Fu, 2001), but in this range the number of stripes is, as a rule, no more than three or four, and their emission intensity decreases as frequency decreases. On the assumption that the "zebra-pattern" is of solar origin, various models were proposed that explained its nature (Kuijpers, 1975; Zheleznyakov and Zlotnik, 1975; Mollwo, 1983; Winglee and Dulk, 1986; Chernov, 1990; Ledenev *et al.*, 2001; Ledenev, Yan, and Fu, 2001; LaBelle *et al.*, 2003; Zlotnik *et al.*, 2003; Jasnov and Karlicky, 2004). However, all of these models proceed from the assumption that the "zebra-pattern" is formed directly in the emission source, i.e. it is determined by an emission generation mechanism. At the same time, it is natural to assume, in our opinion, that in many cases (first of all in meter and decimeter ranges) this structure is formed in the process of radio wave propagation, namely, as a result of interference of rays coming to observer in different paths. Since there are always large-scale regular inhomogeneities in the solar

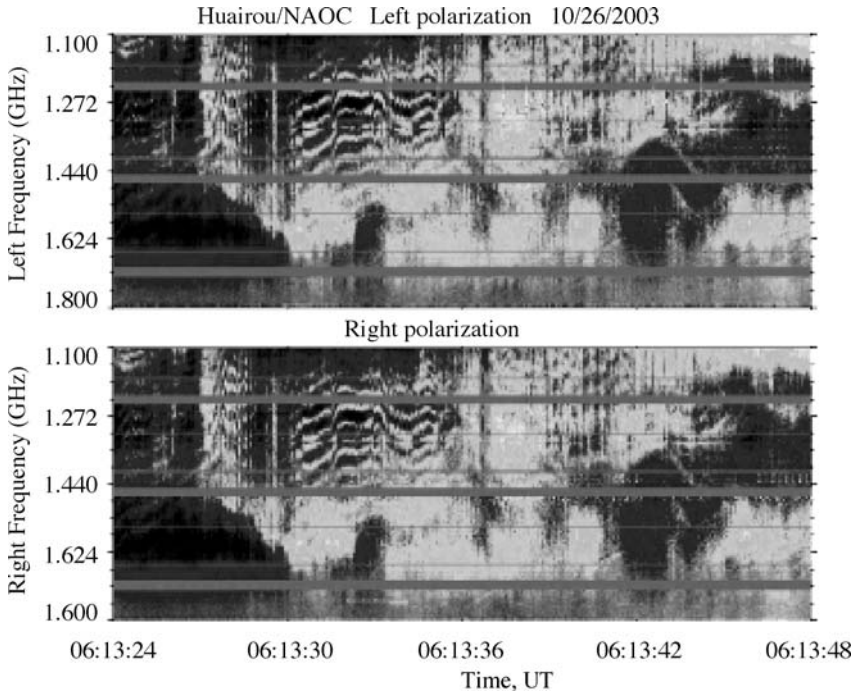

Figure 1. A spectrogram of October 26, 2003 event in decimeter range with the "zebra-pattern" (at the *top* – the left-polarized emission, at the *bottom* – the right-polarized emission) observed with the spectrograph of Beijing Astronomical Observatory.

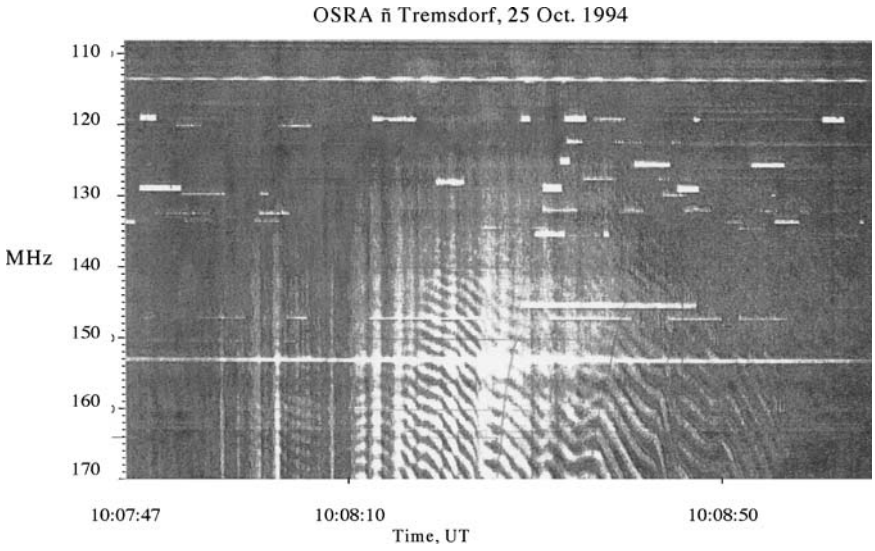

Figure 2. A spectrogram of October 2, 1994 event in meter range with the "zebra-pattern," observed with the spectrograph of Tremsdorf observatory.

corona and emission sources can be considered in many cases as point sources, the emission can propagate from the source to an observer along two paths – direct and reflected. The two rays interfere with each other, and this effect is observed as "zebra-pattern."

2. Formation of "Zebra-Pattern"

In geometrical optics, amplitudes and phases of waves at the observation point are determined by the solution of the ray equation in Hamiltonian form (Felsen and Marcuvitz, 1973; Kravtsov and Orlov, 1980)

$$\mathrm{d}\mathbf{r}/\mathrm{d}\tau = \mathbf{p}, \quad \mathrm{d}\mathbf{p}/\mathrm{d}\tau = (1/2)\nabla n^2(\mathbf{r})$$

and definition of eikonal with the formula

$$\Psi = \Psi_0 + \int_{\tau 0}^{\tau} p^2 \,\mathrm{d}\tau.$$

Here $\mathbf{r}$ is a coordinate along the ray, $\mathbf{p}$ is the wave momentum, n the refractive index, τ is a subsidiary variable connected with the ray length element $\mathrm{d}s$ by the relation $\mathrm{d}\tau = \mathrm{d}s/n$, Ψ_0 is the initial eikonal value for $\tau = \tau_0$s. In a plane-stratified medium, where refractive index n depends only on coordinate z, the ray equation takes the form

$$\mathrm{d}x/\mathrm{d}\tau = p_x, \quad \mathrm{d}y/\mathrm{d}\tau = p_y, \quad \mathrm{d}z/\mathrm{d}\tau = p_z,$$
$$\mathrm{d}p_x/\mathrm{d}\tau = 0, \quad \mathrm{d}p_y/\mathrm{d}\tau = 0, \quad \mathrm{d}p_z/\mathrm{d}\tau = (1/2)\,\mathrm{d}n^2/\mathrm{d}z.$$

Here $p_x = n\sin\theta\cos\phi$, $p_y = n\sin\theta\sin\phi$, $p_z = n\cos\phi$, θ is the angle between the wave vector and the z-axis, ϕ is the angle between the wave vector projected onto the xy-plane and the x-axis. Here $n\sin\theta =$ constant (refraction law) and the angle $\phi =$ constant, i.e. the ray is a planar curve.

As noted earlier, the "zebra-pattern" is usually observed against the background of continuum emission. If the emission source is a point, and at the same time it is broad-band, then an interference structure will form, if the source size is less than the smallest wavelength in the emission spectrum. But the real size of the emission source is much larger than the wavelength, so that the source must be narrow band to keep a phase correlation between direct and reflected waves, i.e. to provide their coherence. The narrow-band emission can be generated by plasma mechanism (Zheleznyakov, 1970) provided that the source size is much less than the density scale height in the corona. In that case the emission source may be considered as a point source, and waves radiated by the source are spherical waves at distances from the source much less than the density scale height L and larger than the source size (Felsen and Marcuvitz, 1973; Kravtsov and Orlov, 1980). But it is not likely that such a small source can provide enough emission flux to form the

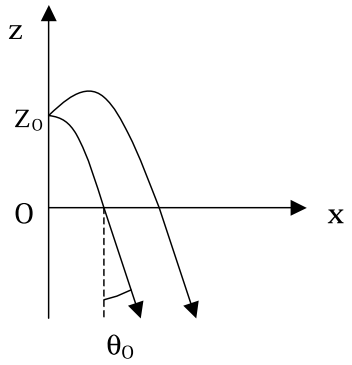

Figure 3. Trajectories of direct and reflected rays from a small source located in an inhomogeneous layer at the point z_0.

"zebra-pattern" against the background of continuum emission. The solution of the problem lies in the assumption that the emission comes from a multitude of discrete narrow-band sources of small size. As it will be shown later, such an assumption agrees with contemporary conception of emission generation by plasma mechanism (Melrose, Dulk, and Cairns, 1986; Robinson, Cairns, and Gurnett, 1992). In this case, we can take $\omega_{pe}/\omega \approx 1$ in every point, and various values of the z-coordinate correspond to different emission frequencies.

Let us suppose that the emission source is situated in a linear inhomogeneous layer (refractive index $n^2(z) = 1 - z/L$) at a distance z_0 from the border of the layer. On the other hand, $n^2 = 1 - \omega_{pe}^2/\omega^2$, i.e. the density in the layer changes in accordance with linear law. The electromagnetic field of the emission source is defined as $u = (B/R_0)\exp(ik_0 n^0 R_0)$. Here $B = \text{constant}$, $n^0 = n(z_0)$, $R_0 = (x_0^2 + z_0^2)^{1/2} \ll L$. The ray geometry is shown in Figure 3. The total field at the observation point consists of the sum of direct and reflected rays from small source as (Kravtsov and Orlov, 1980)

$$\begin{aligned} u(R,\theta) &= A_1 \exp(ik_0\Psi_1) + A_2 \exp(ik_0\Psi_2) \\ &= 2(B/R)\exp(ik_0 R)(\cos\theta)^{1/2}(\cos^2\theta - z_0/L)^{-1/4} \\ &\quad \times \cos[(2k_0 L/3)(\cos^2\theta - z_0/L)^{3/2} - \pi/4] \\ &\quad \times \exp[(i2k_0 L/3)\cos^3\theta - i\pi/4]. \end{aligned} \tag{1}$$

Here $R = (x^2 + z^2)^{1/2}$, $k_0 = \omega/c$. If we suppose that the emission is generated at a frequency close to plasma frequency, then we can take $\omega_{pe}/\omega \approx \text{constant}$, i.e. $\omega_{pe}^2/\omega^2 \approx \omega_{pe\,0}^2/\omega_0^2 \approx z_0/L$. Here $\omega_{pe\,0}$ is the local plasma frequency in the region of emission generation, and ω_0 is the emission frequency in this region. In our case, the radiation is observed at a fixed angle θ from many small sources distributed in the inhomogeneous layer and radiating at different frequencies. The sources are situated at different distances from the border of the inhomogeneous layer. This

assumption is not so essential because the interference picture is determined mainly by the distance from every small source to its ray reflection point. This distance is the same for all the small sources in linear inhomogeneous layer. As evident from Equation (1), when a broad-band emission is observed at a fixed angle θ and at a fixed moment of time, a periodic structure in frequency is observed, which is determined by the factor

$$u(\omega) = \cos\left[(2L\omega/3c)\left(\cos^2\theta - \omega_{\mathrm{pe}\,0}^2/\omega_0^2\right)^{3/2} - \pi/4\right]. \tag{2}$$

Since the parameter $L\omega/c \gg 1$, then generally a period of this structure is very small, and it is beyond the frequency resolution of existing instruments. However, provided that $\cos^2\theta \approx \omega_{\mathrm{pe}\,0}^2/\omega_0^2$, this period increases substantially and may lead to observable values. For example, in the event October 26, 2003 (Figure 1) in the frequency band of about 30%, roughly 10 "zebra-pattern" strips were observed. The plot of emission intensity $u^2(\omega)$ versus frequency is shown in Figure 4 for fixed moment of time, $f \sim 10^9$ Hz (a decimeter-wave range), frequency band $\Delta\omega/\omega \approx 10^{-2}$ and $L \sim 5\times10^8$ cm. Here we take $\cos^2\theta \approx \omega_{\mathrm{pe}\,0}^2/\omega_0^2 \approx 0.98$, i.e. $\theta \approx 8^\circ$. Also for the event in a meter-wave range ($f \sim 10^8$ Hz, frequency band ~20%) we get the structure (Figure 5) with the period corresponding to Figure 2 for $L \sim 5 \times 10^9$ cm and $\cos^2\theta \approx 0.98$. We take the density scale heights L less than that of the quiet solar corona, because typical parameter values of the quiet corona give too large difference between the direct and reflected rays and make the "zebra-pattern" stripes almost merge together. In active regions (especially during flares) such a small density scale height is quite probable due to a complicated structure of the magnetic field.

The change of $\cos\theta$ by 1% gives the change of the angle θ by 1°. This angle is much larger than typical angular sizes of broad-band solar radio sources (Krüger,

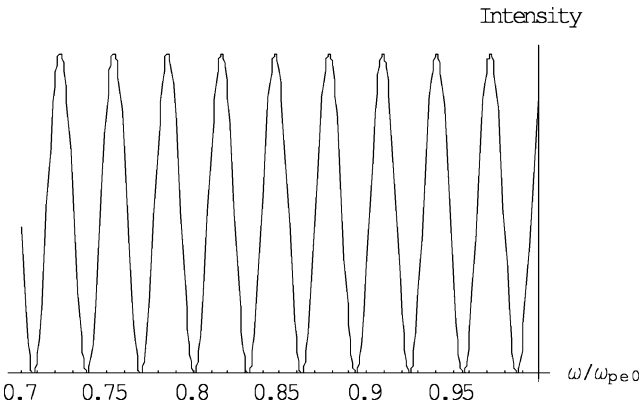

Figure 4. Relative emission intensity expected from a great number of small sources versus frequency in a decimeter-wave range for frequency $f_0 = 10^9$ Hz, spatial scale $L = 5 \times 10^8$ cm and $\theta_0 \approx 8^\circ$. $\omega_{\mathrm{pe}\,0}$ is a plasma frequency in the source with maximum emission frequency.

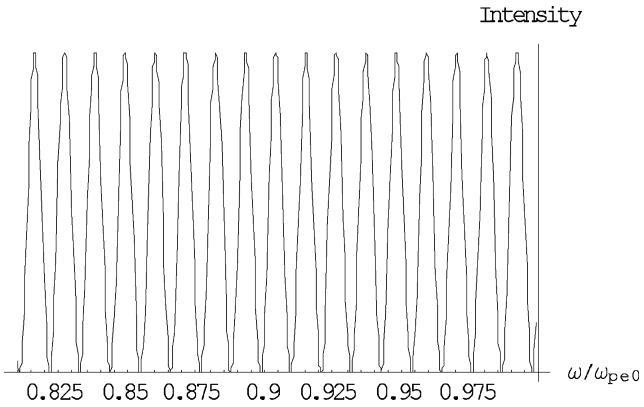

Figure 5. Relative emission intensity expected from a great number of small sources versus frequency in a meter-wave range for frequency $f_0 = 10^8$ Hz, spatial scale $L = 5 \times 10^9$ cm, and $\theta_0 \approx 8^\circ$. $\omega_{\mathrm{pe}\,0}$ is a plasma frequency in the source with maximum emission frequency.

1979). Hence, we can suppose that the radiation comes from one direction, i.e. relation $\cos^2\theta \approx \omega_{\mathrm{pe}\,0}^2/\omega_0^2$ is rather precise, and if we observe the emission at angles, for which this equality is fulfilled, interference strips ("zebra-pattern") arise in the broad-band emission spectrum.

If a matter moves in the source region, i.e. the density gradient changes, the distance between the emission source and the reflection point changes accordingly (therewith the source moves also). This involves the change of the length difference between the direct and reflected rays. If the border of the inhomogeneous layer moves with a speed of $\sim 10^7$ cm s^{-1} (about the sound speed in the corona), then for $L \sim 10^9$ cm the gradient decreases by 10% in a time interval $\Delta t \sim 10$ s, and the "zebra-pattern" shifts approximately by the same amount toward high frequencies as one can see in Figure 2. Such a shift of "zebra-pattern," which is a result of the movement of the medium and the emission source, is observed in reality (Aurass *et al.*, 2003).

The angular width where the "zebra-pattern" is observed (the light cone) is determined by condition $\theta = \arccos(z_0/L)^{1/2}$ (Kravtsov and Orlov, 1980). The deeper the source position in the inhomogeneous layer, the narrower angular width of the cone where the "zebra-pattern" is observed. In our case, $\theta \approx \arccos(\omega_{\mathrm{pe}\,0}/\omega_0)$.

The frequency interval between adjacent strips of "zebra-pattern" is $\sim$1%. Namely a wavelength variation of 1% gives the change in the phase difference between direct and reflected waves of about 180°. This, in turn, means that the path difference in the interfering rays is about 100 wavelengths. Since in our case $\omega \approx \omega_{\mathrm{pe}\,0}$ and $\Delta\omega/\omega \approx 10^{-2}$ the wavelength in the source is $\lambda \sim 10\lambda_0$, i.e. $\lambda \sim 10^3$ cm for meter-range waves. Here λ_0 is the wavelength in the observation point. This means that the path difference between the direct and reflected rays is about 10^5 cm. This

difference is accumulated on the part of the reflected ray trajectory from the source to the reflection point and back. Here it is necessary to keep in mind that the real distance between the emission source and the reflection point is larger than $10^2\lambda$, since the component of wave vector directed along the density gradient tends to zero as the reflection point is approached. At the same time, if the density in the source region is by about 1% less than the density in the reflection point, then the distance from the source to the reflection point is not more than $10^{-2}L$, i.e. less than 10^7 cm for $L \sim 10^9$ cm. Then the emission source size is $l \ll 10^7$ cm, i.e. $l \leq 10^6$ cm.

Hence our calculations show a reasonable explanation for the "zebra-pattern" by an interference of the emission from small ($\leq 10^6$ cm) sources. As a rule, "zebra-pattern" is observed against the background of a broad-band emission with the source size of about 10^9 cm or more (Krüger, 1979). Therefore, it is unlikely for a single source of such a small size to become apparent against the background of the continuum. Therefore, we suggest that the "zebra-pattern" is formed by a great number of small sources, which are clustered in the region of continuum emission. This is in agreement with contemporary idea on the structure of a flare region (Aschwanden, 2002).

Spacecraft observations (Gurnett and Anderson, 1977; Lin *et al.*, 1986) show that Langmuir turbulence in the solar wind is confined in small regions (clumps) right down to the smallest scales that can be resolved. The energy density of the turbulence changes by several orders of magnitude in about 1 s and less. Robinson, Cairns, and Gurnett (1992) show that the spatial size distribution of concentration of Langmuir waves is analogous to the distribution of density fluctuation in the solar wind. They confirmed this prediction by spectral analysis of spacecraft ISEE-3 data.

We suppose that the major contribution to the broad-band emission in meter and decimeter waves (type IV bursts) are provided by plasma mechanism (Stepanov, 1973; Ledenev, 1982). This means that in the emission region a plasma (Langmuir) turbulence is generated, which is then transformed into electromagnetic radiation. It is natural to suppose that, as in the solar wind, the turbulence is concentrated in small regions, i.e. the emission region consists of a great number of small sources (clumps) (Melrose, Dulk, and Cairns, 1986; Robinson, Cairns, and Gurnett, 1992). Such fragmentation of the emission source occurs as a result of plasma waves captured in density minima of background plasma fluctuations. The capture occurs if a variation of plasma frequency in passing from density minimum to maximum $\Delta\omega = (\Delta N/N)\omega_{pe}/2$, exceeds the width of plasma wave spectrum at this place. If we suppose that the waves are excited in the phase velocity interval Δv, then the capture condition is $(\Delta N/N) > 6v_{Te}^2\Delta v/v^3$ (Melrose, Dulk, and Cairns, 1986). Here v is the velocity of energetic electrons, and v_{Te} is the thermal electron velocity. Hence, the estimated maximum size of the clumps is $l_{max} \approx 3Lv_{Te}^2\Delta v/2v^3$ (Robinson, Cairns, and Gurnett, 1993). Here L is the spatial scale of density in emission region. For $\Delta v \approx v$, $v_{Te} \approx 0.1v$, $L \approx 10^8$ cm we get $\Delta N/N \approx 0.06$, $l_{max} \approx 0.01L \approx 10^6$ cm, i.e. the spatial scale of clumps $l \leq 10^6$ cm.

If we take $L \approx 10^9$ cm, then with the other parameters being the same, the spatial sizes of density fluctuations are mainly in the region $l \leq 10^7$ cm.

For the existence of stable interference patterns, the lifetime of the clumps has to be much less than the time scale of variations in the background plasma parameters, which determine the temporal behavior of "zebra-pattern" as a whole. As one can see from Figures 1 and 2, the time scale of these variations is about 1 s and more. This means that the lifetime of the clumps is about 0.1 s or less.

Phase relations between the direct and reflected rays are more stable at low frequencies, since the background plasma parameters vary more smoothly with space and time at higher layers in the corona. In particular, this explains that the "zebra-pattern" is observed in meter waves more often than in decimeter-wave and especially in microwave ranges. Correspondingly, the duration of "zebra-pattern" decreases as the frequency increases, from tenth of a second in meter waves to several seconds in decimeter waves (Figures 1 and 2).

Electromagnetic radiation is generated at frequency close to the plasma frequency as a result of linear conversion of plasma waves into electromagnetic waves (Zheleznyakov, 1970). Plasma waves captured in a density minimum are transformed into electromagnetic waves as they approach the reflection point, where the wave number of plasma wave decreases and matches the wave number of electromagnetic wave. The direction of the wave vector of plasma wave therewith is close to the direction of the density gradient in the clump, and the direction of the wave vector of electromagnetic wave is almost perpendicular to the gradient direction. Usually, density fluctuations are stretched out along the magnetic field (Melrose, Dulk, and Cairns, 1986). This means that the emission escapes from the clump mainly along the magnetic field due to less stringent capture conditions. The emission from every clump is narrow band with $\Delta\omega/\omega \approx 3v_{\mathrm{Te}}^2 \Delta v/v^3$ (Melrose, Dulk, and Cairns, 1986), i.e. $\Delta\omega/\omega \approx 1\%$ for the parameter values taken earlier.

The emission at frequency close to plasma frequency in decimetric range is strongly absorbed due to Coulomb collisions (Benz, 1993). But sometimes the emission at the fundamental frequency is observed in a decimeter range (Benz, 1993; Ledenev *et al.*, 2001). It is possible if the emission is intensive enough and density scale height is small enough (in our case $L \sim 5 \times 10^8$ cm).

The "zebra-pattern" is observed as a broad-band emission, if the emission source occupies an extended region, in which the maximum number of clumps along the density gradient is about $\omega_{\mathrm{pe}}/\Delta\omega \sim 10^2$. The brightness temperature of the (optically thick) discrete sources giving rise to the "zebra-pattern," relative to the temperature of the background source (type IV burst), is determined by a filling factor, i.e. the ratio of the sum of the areas occupied by the discrete sources at a fixed level to the area of continuum source. For example, if the filling factor is about 1%, then for brightness temperature of type IV burst $\sim 10^8$ K, the temperature of the discrete source is $\sim 10^{10}$ K. If we take into account the wave damping during its propagation, the temperature is 1 order of magnitude higher. If the brightness temperature or the filling factor is less than these values, the modulation factor of

"zebra-pattern" will be below unity. A small filling factor will provide almost free propagation of electromagnetic waves because the waves come in the region with $n \approx 1$ without considerable scattering by other clumps.

3. Conclusion

Our calculations show that the "zebra-pattern" in continuum solar emission in meter and decimeter ranges can be formed as an interference of direct and reflected rays from a small source. The observed flux of radio emission can be explained by summing fluxes from a great number of such sources. The emission is generated by plasma mechanism, i.e. plasma instability excites plasma waves, which then transform into plasma radiation.

The "zebra-pattern" in broad-band solar radio emission is observed when the relation $\cos^2\theta \approx \omega_{\mathrm{pe}\,0}^2/\omega_0^2$ is fulfilled between the angle θ of emission emergence from inhomogeneous layer relative to the density gradient and the ratio of plasma frequency in the emission source to the emission frequency is close to unity. This condition can be fulfilled in the event of plasma mechanism in meter and decimeter waves for small enough angles θ only, namely for $\theta < 10^\circ$.

The observed flux of emission is created by a great number of discrete sources corresponding to local density minima with captured Langmuir waves. The size of discrete emission sources is $\leq 10^6$ cm and the bandwidth is $\sim 1\%$.

Acknowledgements

We thank H. Aurass and G. Chernov for providing the meter range data. The work was supported by the Russian Foundation for Basic Research and State Foundation for Natural Sciences of China(grants 03-02-16229, 04-02-39003).

References

Aschwanden, M. J.: 2002, *Space Sci. Rev.* **101**, 1.
Aurass, H., Klein, K.-L., Zlotnik, E. Y., and Zaitsev, V. V.: 2003, *Astron. Astrophys.* **410**, 1001.
Benz, A. O.: 1993, *Plasma Astrophysics*, Kluwer Academic Publishers, Dordrecht.
Chernov, G. P.: 1976, *Soviet Astron.* **20**, 582.
Chernov, G. P.: 1990, *Solar Phys.* **130**, 75.
Elgarøy, O.: 1959, *Nature* **184**, 887.
Felsen, L. B. and Marcuvitz, N.: 1973, *Radiation and Scattering of Waves*, Prentice-Hall, New Jersey.
Gurnett, D. A. and Anderson, R. R.: 1977, *J. Geophys. Res.* **82**, 632.
Izliker, H. and Benz, A. O.: 1994, *Astron. Astrophys.* **104**, 145.
Jasnov, L. V. and Karlicky, M.: 2004, *Solar Phys.* **219**, 289.

Kravtsov, A. Y. and Orlov, Y. I.: 1980, *Geometrical Optics of Inhomogeneous Medium*, Moscow, Nauka (in Russian).
Krüger, A.: 1979, *Introduction to Solar Radio Astronomy and Radio Physics*, D. Reidel, Dordrecht.
Kuijpers, J.: 1975, *Solar Phys.* **44**, 173.
Kundu, M. R.: 1965, *Solar Radio Astronomy*, Interscience, New York.
LaBelle, J., Treumann, R. A., Yoon, P. H., and Karlicky, M.: 2003, *Astrophys. J.* **593**, 1195.
Ledenev, V. G.: 1982, *Soviet Astron.* **26**, 452.
Ledenev, V. G., Karlicky, M., Yan, Y., and Fu, Q.: 2001, *Solar Phys.* **202**, 71.
Ledenev, V. G., Yan, Y., and Fu, Q.: 2001, *Chin. J. Astron. Astrophys.* **1**, 475.
Lin, R. P., Levedahl, W. K., Lotko, W., Gurnett, D. A., and Scarf, F. L.: 1986, *Astrophys. J.* **308**, 954.
Melrose, D. B., Dulk, G. A., and Cairns, I. H.: 1986, *Astron. Astrophys.* **163**, 229.
Mollwo, L.: 1983, *Solar Phys.* **83**, 305.
Ning, Z., Fu, Q., and Lu, Q.: 2000, *Astron. Astrophys.* **364**, 793.
Robinson, P. A., Cairns, I. H., and Gurnett, D. A.: 1992, *Astrophys. J.* **387**, L101.
Robinson, P. A., Cairns, I. H., and Gurnett, D. A.: 1993, *Astrophys. J.* **407**, 790.
Slottje, C.: 1972, *Solar Phys.* **25**, 210.
Stepanov, A. V.: 1973, *Soviet Astron.* **17**, 781.
Winglee, R. M. and Dulk, G. A.: 1986, *Astrophys. J.* **307**, 808.
Zheleznyakov, V. V.: 1970. *Radio Emission of the Sun and Planets*, Pergamon Press, Oxford.
Zheleznyakov, V. V. and Zlotnik, E. Y.: 1975, *Solar Phys.* **44**, 431.
Zlotnik, E. Y., Zaitsev, V. V., Aurass, H., Mann, G., and Hofmann, A.: 2003, *Astron. Astrophys.* **410**, 1011.